

Domain walls and Schramm-Loewner evolution in the random-field Ising model

Jacob D. Stevenson¹ and Martin Weigel¹

¹*Institut für Physik, Johannes Gutenberg-Universität Mainz, Staudinger Weg 7, 55128 Mainz, Germany*

(Dated: November 3, 2018)

The concept of Schramm-Loewner evolution provides a unified description of domain boundaries of many lattice spin systems in two dimensions, possibly even including systems with quenched disorder. Here, we study domain walls in the random-field Ising model. Although, in two dimensions, this system does not show an ordering transition to a ferromagnetic state, in the presence of a uniform external field spin domains percolate beyond a critical field strength. Using exact ground state calculations for very large systems, we examine ground state domain walls near this percolation transition finding strong evidence that they are conformally invariant and satisfy the domain Markov property, implying compatibility with Schramm-Loewner evolution (SLE _{κ}) with parameter $\kappa = 6$. These results might pave the way for new field-theoretic treatments of systems with quenched disorder.

In the past decades, analytic techniques such as conformal field theory (CFT) and Coulomb gas methods have led to a rather comprehensive understanding of critical phenomena in two dimensions (2D). In particular, CFT allows for a complete classification of 2D critical points, the exact determination of critical exponents and, in some cases, even scaling amplitudes [1]. This success is tied to the fact that the conformal group is infinite-dimensional, however, which is true only in 2D, and few of the results generalize to higher dimensions [2]. Another difficulty for this approach arises for the important class of systems with quenched disorder, such as diluted magnets, random-field systems and spin glasses [3], since the non-unitary CFTs that are believed to describe systems with quenched disorder are poorly understood [4].

While some geometrical aspects of critical phenomena had been previously worked out using concepts from the Coulomb gas [5] and two-dimensional quantum gravity [6], a breakthrough was achieved with the description of domain boundaries in terms of random curves in the plane in a framework dubbed Schramm-Loewner evolution (SLE) [7]. In SLE, stochastic curves in the plane are constructed from one-dimensional Brownian motion, thus classifying a statistical ensemble of curves with only one parameter, the diffusion constant κ . Characteristic interfaces in many physical systems have been shown (in some cases rigorously) to satisfy SLE _{κ} . These include percolation ($\kappa = 6$), self avoiding walks ($\kappa = 4/3$), as well as spin cluster boundaries ($\kappa = 3$) and Fortuin-Kasteleyn cluster boundaries ($\kappa = 16/3$) in the Ising model. In recent years, close connections between SLE and CFT, including links between probabilistic properties of SLE curves and scaling operators in CFT, or between the central charge c of the CFT and the diffusion constant κ have been established [7]. A number of numerical studies have found interfaces in disordered systems to be (partially) consistent with SLE, in particular the 2D Ising spin glass [8, 9], the Potts model on dynamical triangulations [10], the random bond Potts model [11], and the disordered solid-on-solid model [12]. Such findings and the close link between SLE and CFT spur the hope of a more complete understanding of systems with quenched disorder from a field-theoretic perspective.

I. RANDOM-FIELD ISING MODEL

Here, we study domain walls in the random-field Ising model (RFIM) with Hamiltonian [13]

$$\mathcal{H} = -J \sum_{\langle i,j \rangle} s_i s_j - \sum_i h_i s_i, \quad (1)$$

where the spins $s_i = \pm 1$ are located on the sites of a square lattice and interact ferromagnetically with nearest neighbors. The local fields h_i are quenched random variables which, for the time being, we take as drawn from a Gaussian distribution with mean H and standard deviation Δ . Since only the ratio J/Δ is relevant, we take $J = 1$. Random field models have a large number of experimental realizations which are of technological importance such as superfluid helium, liquid crystals in silica aerogels, Bragg glasses in high- T_c superconductors, amorphous solids [14] and ferroelectric materials [15]. It was shown by Imry and Ma [16] that random fields destabilize the ferromagnetic order in dimensions $d \leq 2$. For the case of 2D, it was argued by Binder [17] that ferromagnetic order occurs only up to a break-up length scale $L_b \sim e^{A/\Delta^2}$, which grows with decreasing disorder Δ , and that the system remains paramagnetic at scales $L > L_b$. Later, Aizenman and Wehr [18] proved that for $d \leq 2$ the system indeed has a unique Gibbs state, precluding the existence of an ordering transition. On the contrary, for $d \geq 3$, L_b diverges at the thermodynamic transition point, below which the system is ferromagnetic [13]. For non-zero average fields H , on the other hand, even in 2D the size of spin clusters diverges at a critical value $H_c = H_c(\Delta)$ [19–22]. However, the weight of these clusters is sub-extensive, such that the free energy remains analytic and no thermodynamic phase transition occurs. This phenomenon bears many similarities to the Kertész line in ferromagnets in the absence of disorder [23]. It is this transition at non-zero H that we study in this Letter.

To investigate the properties of domain walls in the RFIM we numerically compute exact ground states of samples of random-field realizations. Ground states can be found in polynomial time via a mapping to a minimum-cut/maximum-flow problem [24]. We employ a fast algorithm based on the idea of “augmenting paths” [25], which allows us to find ground states of systems of 10^7 spins in about 6 s, such that the maxi-

imum system sizes exceed those of previous studies [19–21] by about an order of magnitude. We use a variety of domain geometries, partially with fixed spins to enforce the occurrence of domain walls. The calculations reported here were carried out at either $\Delta = 2.5$ and $H = 0.01362 = H_c(\Delta) \pm 0.00007$ or at $\Delta = 1.7$ and $H = 5.08 \times 10^{-4} = H_c(\Delta) \pm 0.07 \times 10^{-4}$. For both cases the breakup length scale is only a few lattice spacings, much less than the system sizes we look at. Both the breakup length scale and the critical external field were determined using recipes laid out in Ref. [20].

II. SCHRAMM LOEWNER EVOLUTION

In the framework of Loewner evolution one imagines a random curve γ_t in the plane as being continuously grown in time t in a random process. Instead of studying this process directly, one considers the evolution of a family $g_t : \mathbb{H} \setminus \gamma_t \rightarrow \mathbb{H}$ of conformal maps that take the complement of γ_t in the upper half plane \mathbb{H} to \mathbb{H} . Under this map the curve γ_t , which lies on the boundary of $\mathbb{H} \setminus \gamma_t$, is taken to the boundary of \mathbb{H} , i.e. to the real line. Assuming standard normalization and boundary conditions, it turns out that g_t is completely determined by the one-dimensional function ξ_t , which corresponds to the image under g_t of the tip of the growing curve on the real line, via the differential equation

$$\frac{\partial g_t(z)}{\partial t} = \frac{2}{g_t(z) - \xi_t}. \quad (2)$$

It was shown by Schramm [26] that if the ensemble of curves γ_t is conformally invariant and satisfies the domain Markov property (to be discussed below), the one-dimensional random process described by ξ_t must be Brownian motion with zero mean and variance κt . For such SLE curves, many stochastic properties can be calculated rigorously including, for instance, the fractal dimension $d_f = 1 + \kappa/8$ or the probability $P_{\text{LP}}(x, y)$ that the curve γ_t passes to the left of the point (x, y) . The latter was proven by Schramm [27] for curves starting at the origin of the upper half plane \mathbb{H} to be

$$P_{\text{LP}}^\kappa(x, y) = \frac{1}{2} + \frac{\Gamma(4/\kappa)}{\sqrt{\pi} \Gamma(\frac{8-\kappa}{2\kappa})} \frac{x}{y} {}_2F_1\left(\frac{1}{2}, \frac{4}{\kappa}; \frac{3}{2}; -\left(\frac{x}{y}\right)^2\right) \quad (3)$$

where ${}_2F_1$ is Gauss' hypergeometric function.

III. DOMAIN MARKOV PROPERTY

The domain Markov property (DMP) formalizes the notion that a growing path of the type described above is agnostic about its past. Let $P_{\mathbb{D}}(\gamma_{ab})$ be the probability measure of curves γ_{ab} in a domain \mathbb{D} running between points a and b on the boundary of \mathbb{D} , and let c be a point in the interior of \mathbb{D} . Then, the DMP states that

$$P_{\mathbb{D}}(\gamma_{cb}|\gamma_{ac}) = P_{\mathbb{D} \setminus \gamma_{ac}}(\gamma_{cb}), \quad (4)$$

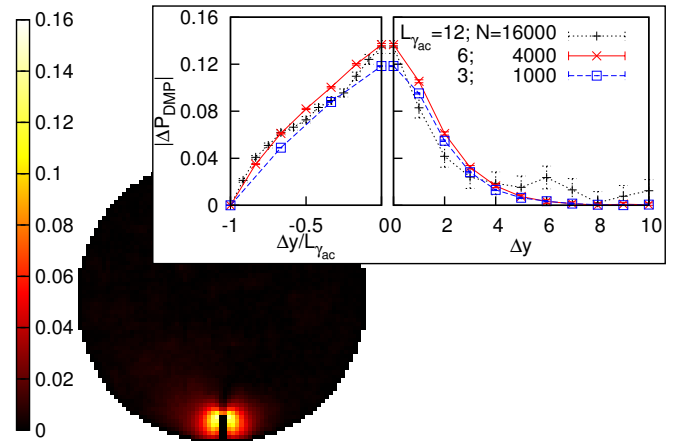


FIG. 1. (Color online) The main panel shows the spatial distribution of $|\Delta P_{\text{DMP}}(x, y)|$ for a system of 4000 spins in a circular domain and a vertical cut γ_{ac} of length 6 starting at the bottom of the domain. Lighter colors correspond to larger deviations from the DMP. The right inset panel shows the decay of $|\Delta P_{\text{DMP}}(35, y)|$ with distance in the positive vertical direction Δy (in lattice spacings) from the point of maximum deviation. Three different system sizes and correspondingly scaled cut lengths γ_{ac} are shown. The left inset panel shows the decay in the negative vertical direction (i.e. along the cut) vs. Δy scaled by the cut length. The tests were performed at $\Delta = 2.5$ and $H = 1.362 \times 10^{-2} \approx H_c(\Delta)$.

i.e., the probability of γ_{cb} is independent of whether γ_{ac} is preconditioned in domain \mathbb{D} , or whether γ_{ac} is excluded from the domain itself. While it is not debated that the DMP holds for domain boundaries in pure lattice systems [7], even off criticality, it has been argued that it is likely not to survive the average over quenched disorder [9]. For the RFIM, we have checked the DMP numerically using the left passage probabilities $P_{\text{LP}}(x, y)$ instead of calculating the probability of all possible curve segments γ_{cb} . For the l.h.s. of Eq. (4), this amounts to picking out those configurations of the random fields that yield an interface along γ_{ac} , while for the r.h.s., the interface is asserted to run along γ_{ac} , for instance by fixing the corresponding spins with large magnetic fields. If the DMP holds, then

$$\begin{aligned} \Delta P_{\text{DMP}}(x, y) &= \sum_{\gamma_{cb}} P_{\mathbb{D}}(\gamma_{cb}|\gamma_{ac}) P_{\text{LP}}(x, y; \gamma_{cb}) \\ &\quad - \sum_{\gamma_{cb}} P_{\mathbb{D} \setminus \gamma_{ac}}(\gamma_{cb}) P_{\text{LP}}(x, y; \gamma_{cb}) \end{aligned} \quad (5)$$

will be identically zero. We have studied system sizes of 1000, 4000, and 16 000 spins with proportionally scaled cuts γ_{ac} of length 3, 6, and 12, respectively. For the largest system, we looked at 3×10^8 ground state configurations, of which only about 2800 satisfied the conditioning along γ_{ac} . As is clearly seen from $|\Delta P_{\text{DMP}}(x, y)|$ shown in the main panel of Fig. 1, the DMP does not survive the disorder average exactly. The deviations are maximal around the tip of γ_{ac} and fall off rapidly with distance from γ_{ac} . As shown in the right inset panel the decay of ΔP_{DMP} with the vertical offset Δy from the tip of γ_{ac} is nearly independent of the system size and the

length of γ_{ac} . In contrast, as shown in the left inset, the decay rate for $\Delta y < 0$, i.e., along the cut, is proportional to the cut length. Perpendicular to the cut, the decay rate (not shown) is again independent of system size. Hence, the intrusion of deviations into the interior of the domain extends to only a few lattice spacings and is largely independent of system size and cut length, such that the DMP will be recovered in the scaling limit. We find that the agreement with the DMP in the scaling limit also holds off the critical percolation line.

IV. LEFT PASSAGE PROBABILITY

We examined the agreement of the RFIM interfaces with the SLE expectations for the left passage probabilities. As the rigorous result of Eq. (3) is valid on the upper half plane \mathbb{H} , we performed our ground state calculations on lattices embedded in domains \mathbb{D} which have simple, closed-form conformal maps $w(z)$ to \mathbb{H} [12]. By fixing the boundary spins through the respective random fields, the interface was forced to run between points a and b in \mathbb{D} which are mapped to the origin and infinity in \mathbb{H} , respectively. Numerical checks were performed for the unit circle with the interface between $-i$ and i , which is mapped to \mathbb{H} by $w(z) = i\frac{1+z}{1-z}$, as well as the unit square with interfaces defined from 0 to $1+i$, which is mapped to \mathbb{H} by $w(z) = -\wp(1+i-z; 1, i)$ where $\wp(z; w_1, w_2)$ is the Weierstrass p-function. Looking at the left passage probability for multiple domains additionally acts as a check of conformal invariance. For a quantitative comparison we considered the mean square deviation of the computed left passage probability P_{LP} from the exact result P_{LP}^κ of Eq. (3),

$$E(\kappa) = \left\langle [P_{LP}(x, y) - P_{LP}^\kappa(x, y)]^2 \right\rangle_{\mathbb{D}}^{1/2}, \quad (6)$$

where $\langle \cdot \rangle_{\mathbb{D}}$ denotes a spatial average over \mathbb{D} , excluding the vicinity of the fixed boundary spins. This quantity is shown in Fig. 2 as a function of κ for the circle and square geometries. In both cases $E(\kappa)$ is minimal for κ within 0.05 of the value $\kappa = 6$. The spatial dependence of the deviation from $P_{LP}^{\kappa=6}(x, y)$ is also shown in Fig. 2 and, for a horizontal cut through the domain, in Fig. 3. There appears to be no systematic deviation.

V. CROSSING PROBABILITY

From the presented results it is evident that spin domain interfaces in the 2D RFIM satisfy the domain Markov property and are conformally invariant at the percolation threshold $H = H_c(\Delta)$ in the scaling limit, and thus are described by SLE. Furthermore, the parameter κ appears to be consistent with $\kappa = 6$ to high precision. To corroborate these findings, we tested our results for compatibility with the exact formulas for the crossing probabilities of percolation clusters, another system with $\kappa = 6$ [28]. These give the probability of finding a cluster of a given species (say up spins) which touches two non-adjacent segments of the boundary of a domain. In particular, the probability π_r of a domain touching

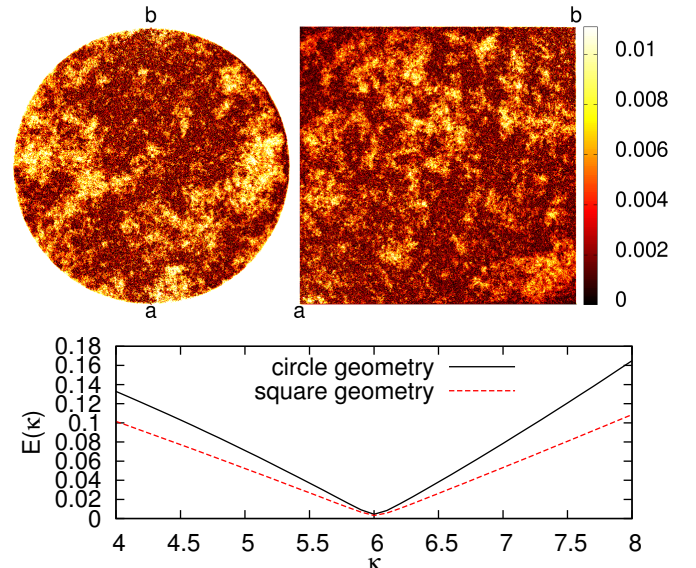


FIG. 2. Magnitude of deviation of the left passage probability for spin domain interfaces from the exact result of Eq. (3) for $\kappa = 6$ in circular and square domains. The interfaces are constrained to run between points a and b as shown. The lower panel displays the spatially averaged deviation $E(\kappa)$ as a function of the diffusion constant κ , showing a clear minimum close to $\kappa = 6$. Calculations were performed for 10 000 disorder realizations on systems of 6×10^6 spins at $\Delta = 2.5$ and $H = 1.362 \times 10^{-2} \approx H_c(\Delta)$.

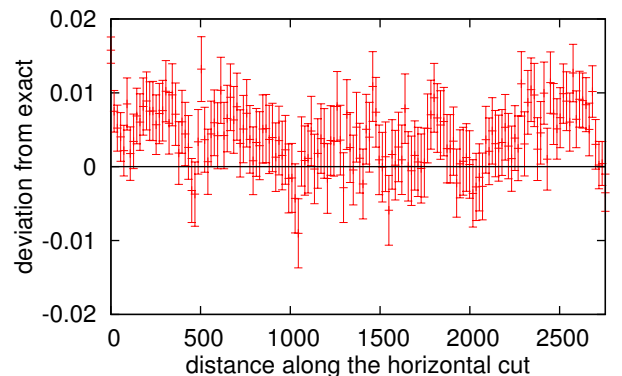


FIG. 3. Deviation from the exact left passage probability along a horizontal line crossing the center of the circle geometry that is shown in Fig. 2.

both the top and bottom of a rectangle of aspect ratio r is known to depend only on r [28]. Similarly, in a domain defined by an equilateral triangle, the probability of a cluster crossing from a fraction x of one boundary edge to the opposite edge is $\pi_x = x$ [29] (see Fig. 4 for a schematic representation). Figure 4 shows these exact percolation results together with numerical simulation data for the RFIM at $\Delta = 1.7$ and $H = 5.08 \times 10^{-4} \approx H_c(\Delta = 1.7)$ for a system of 6×10^6 spins for both the rectangle and triangle geometries. We find very good agreement with the percolation results, cf. the lower panel of Fig. 4. We also show results calculated with an external field $H = 4.71 \times 10^{-4} \approx 0.93 H_c$. Systematic deviations

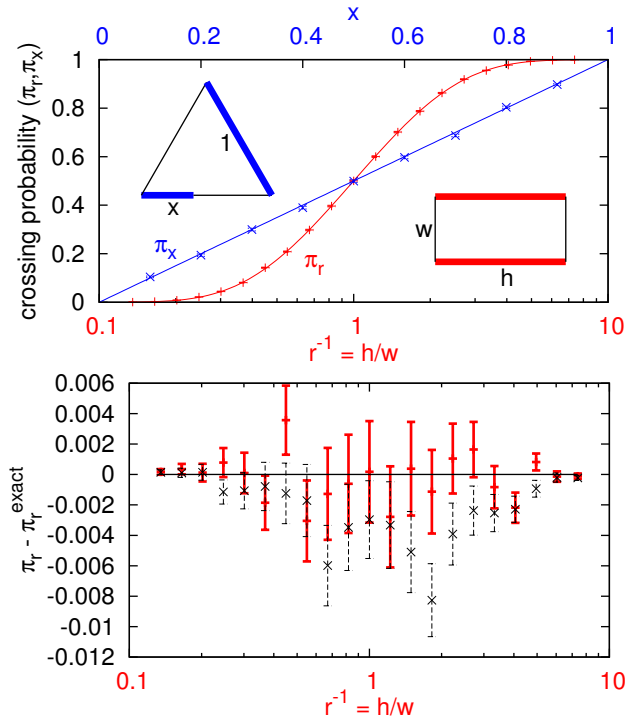


FIG. 4. Upper panel: Crossing probabilities for spin clusters in the 2D RFIM in rectangular (lower scale) and triangular (upper scale) domains. Calculations were performed at $\Delta = 1.7$ and $H = 5.08 \times 10^{-4} \approx H_c(\Delta)$ for $20\text{--}30 \times 10^3$ disorder realizations for the rectangular domain and 7×10^3 realizations for the triangular domain. The solid lines indicate the exact results for percolation clusters ($\text{SLE}_{\kappa=6}$) derived in Refs. [28, 29]. Lower panel: Deviations of the numerical results from the exact expression for percolation for the rectangular domain. Deviations in the triangular domain are similar. Shown with dashed error bars are data calculated at $\Delta = 1.7$, but at an external field $H = 4.71 \times 10^{-4}$. Some systematic deviations from SLE expectations are already seen for this slight detuning from criticality.

from SLE can be clearly seen, even for this slight detuning from criticality, indicating the high sensitivity of our tests.

VI. FRACTAL DIMENSION

One of the rigorous results for curves described by SLE_κ is their fractal dimension, which is given, for $\kappa \leq 8$, by $d_f = 1 + \kappa/8$. We numerically determined the fractal dimension for a range of different geometries and display the results in Fig. 5. We find that corrections to scaling for the interface length L_I are well described by the form

$$L_I = aL^{d_f}(1 + b/L). \quad (7)$$

We take L as the square root of the number of spins for the case of non-rectangular domains. For the circle geometry we find $d_f = 1.7506(9)$, while for the square geometry we arrive at $d_f = 1.7514(14)$, using $\Delta = 2.5$ and $H = 1.362 \times 10^{-2} \approx H_c(\Delta)$ in both cases. These results are perfectly compatible with $d_f = 7/4 = 1.75$ expected for SLE curves with $\kappa = 6$.

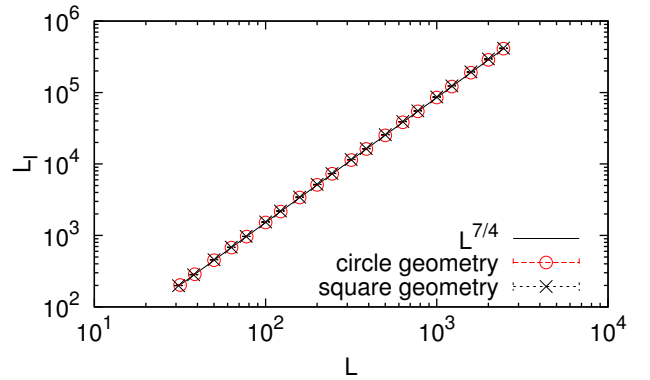


FIG. 5. Scaling of interface lengths with system size. The best fit values — $d_f = 1.7506(9)$ for the circle geometry and $d_f = 1.7514(14)$ for the square geometry — are in excellent agreement with the value expected for SLE_6 , $d_f = 7/4$. The calculations were carried out at $\Delta = 2.5$ and $H = 1.362 \times 10^{-2} \approx H_c(\Delta)$.

VII. BROWNIAN MOTION

As the most direct test for SLE, we studied the one-dimensional stochastic process (or driving function) ξ_t generated by the Loewner map g_t according to Eq. (2) as applied to domain walls in the RFIM. For a lattice system, the family of maps g_t is realized as a discrete series of maps g_i iteratively removing a small section from the beginning of the curve. For this purpose, g_i is approximated using a vertical slit map [30]

$$g_i(z) = i\sqrt{-(z - \xi_i)^2 - 4\Delta t_i} + \xi_i. \quad (8)$$

Here, ξ_i and Δt_i are determined through $\xi_i = x_{i,i-1}$ and $\Delta t_i = y_{i,i-1}^2/4$, where $x_{i,i-1}$ and $y_{i,i-1}$ are the coordinates of the i 'th segment of the curve after undergoing the $i-1$ successive maps $g_{i-1} \circ \dots \circ g_1$. The parameter ξ_i is the value of the driving function ξ_t sampled at time $t_i = \sum_{j \leq i} \Delta t_j$. The complex square root in Eq. (8) is calculated, as usual, with the branch cut along the negative real axis. We studied the statistics of 10 000 interfaces generated in a half disc, optimally mimicking the full space \mathbb{H} . The interface is initiated at the origin by two fixed spins and is considered ended when it touches the curved boundary. We used systems of 6 million spins at $\Delta = 2.5$ and $H = 1.362 \times 10^{-2} \approx H_c(\Delta)$. We find that the variance of the driving function calculated from the interfaces is $\hat{\kappa} = \langle (\xi_t - \langle \xi_t \rangle)^2 \rangle / t = 6.086(87)$, and the normalized mean is $\hat{\xi} = \langle \xi_t \rangle / \sqrt{\hat{\kappa} t} = 0.017(10)$, perfectly compatible with $\text{SLE}_{\kappa=6}$. Using a Kolmogorov-Smirnov test [30, 31], we further checked that the ξ_t are normally distributed and find a p -value of $p = 0.17$, indicating consistency with a normal distribution. To check for the statistical independence of the increments of ξ_t , we divided ξ_t into n increments evenly spaced in time and checked whether the signs of these increments follow a χ^2 distribution with $2^n - 1$ degrees of freedom [30]. For $n = 10$, we find a p -value of $p = 0.18$ indicating consistency with the assumption of statistical independence. As a further check of conformal invariance, we performed the same tests on interfaces originating in the two domains of Fig. 2, and found similar agreement with SLE.

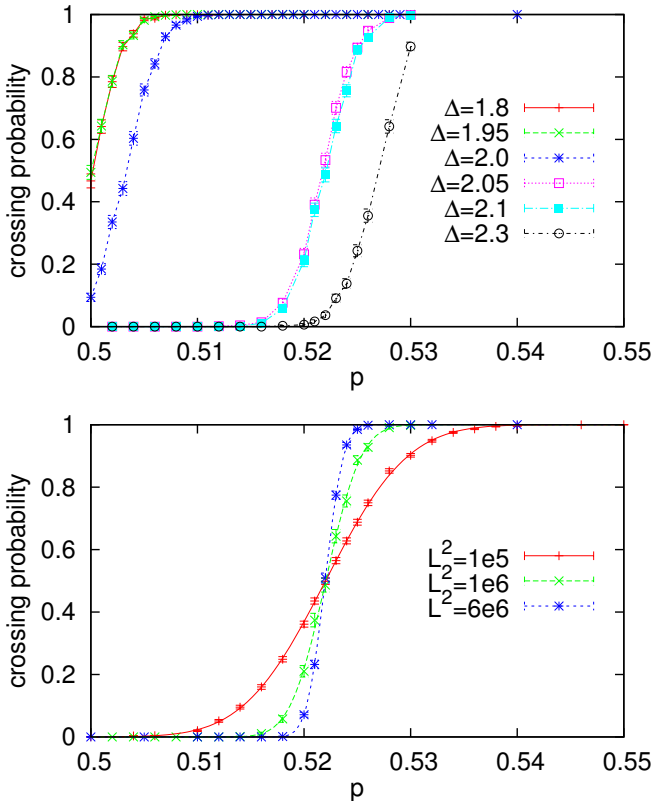


FIG. 6. Crossing probabilities for the binary distribution of fields as a function of the fraction p of up fields. The upper panel shows the dependence of these curves on disorder strength (for system size $L^2 = 10^6$). The bottom panel shows the crossing of these curves for different system sizes at the critical point p_c (at disorder strength $\Delta = 2.1$).

VIII. BINARY FIELDS

Finally, we also considered a binary (Bernoulli) field distribution, where each local random field h_i takes on the value Δ with probability p and $-\Delta$ with probability $1 - p$. Because of the discrete nature of the distribution, this system has a massive ground-state degeneracy, and behaves rather differently from the Gaussian RFIM, at least at zero temperature. Although polynomial algorithms for enumerating all ground states are known [32], handling all ground states becomes impractical for larger system sizes. Here, instead, we sample from the ground-state manifold by adding a tiny noise term (normally distributed with strength δ) to the Bernoulli field distribution. For sufficiently small δ , the resulting state is also a ground state of the noise-less system, and, importantly, is selected without bias from among the degenerate ground states. We find that there exists a geometric transition where spin clusters diverge at $p = p_c(\Delta)$, in analogy with $H_c(\Delta)$ for the Gaussian case. This is illustrated in Fig. 6, where we have plotted, for a number of different disorder strengths, the probability of finding a spin-up cluster that touches both the top and bottom boundaries of a square geometry. Shown in the bottom panel is the size dependence of these curves,

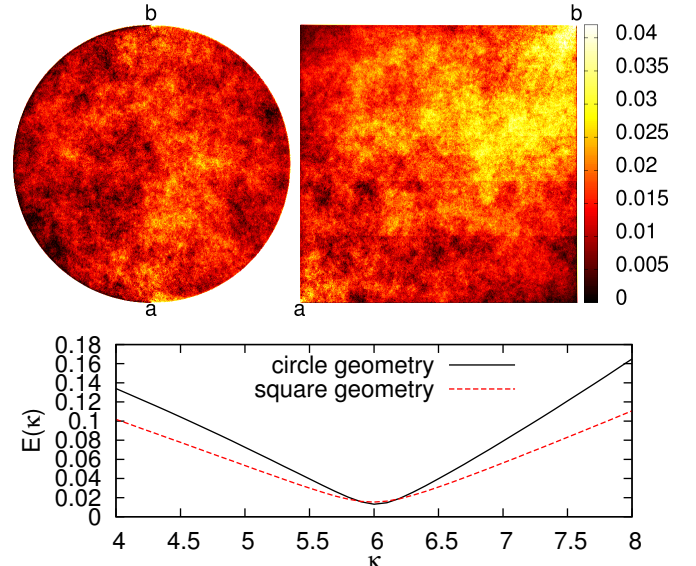


FIG. 7. Left passage probabilities for the binary distribution of fields. See Fig. 2 for a detailed description of the setup. The calculations were carried out at $\Delta = 2.1$ and $p = 0.522 \approx p_c(\Delta)$ for systems of 6 million spins. Averages were performed over 10 randomly chosen ground states for each of 6000 disorder configurations.

demonstrating that different sizes cross at p_c . We also point out that this crossing of curves happens when the crossing probability is 0.5 as expected. Interestingly, as can be seen in the upper panel of Fig. 6, for $\Delta < 2$ this transition appears to occur at the constant value $p_c(\Delta < 2) = 1/2$, while $p_c(\Delta \geq 2) > 1/2$. We test agreement with SLE predictions by looking at the fractal dimension at p_c , finding $d_f = 1.746(2)$, and by looking at the left passage probability, the results of which are shown in Fig. 7. Both properties are consistent with SLE for $\kappa = 6$.

IX. CONCLUSIONS

We have studied the properties of spin cluster interfaces in the ground state of the Gaussian random field Ising model at values of the external field strength H where the size of the clusters diverges. For this $T = 0$ system with quenched disorder, the domain Markov property was shown to be satisfied in the scaling limit. Together with the conformal invariance of the interfaces deduced from Schramm's formula and the crossing probabilities, it is shown clearly that the spin domain interfaces satisfy $\text{SLE}_{\kappa=6}$, corresponding to pure percolation. The fractal dimension is in perfect agreement with these observations, contrary to the case of the solid-on-solid model studied in Ref. [12], where $\kappa \approx 4$ was found from Schramm's formula, but $d_f \approx 1.25 \neq 1 + \kappa/8$. Studying the SLE map directly, we have shown that the driving function describes Brownian motion. The consistency with SLE carries over to the case of binary random fields, where degeneracies occur. This is in contrast to the observations for the spin glass model, where domain walls appear to be only described by SLE for

continuous disorder distributions [8, 9, 33]. The 2D RFIM thus seems to provide a paradigmatic example where SLE is realized in all known aspects in a system with quenched disorder, nourishing the hope for a more systematic treatment of systems with quenched disorder in field theory.

The authors acknowledge computer time provided by NIC Jülich under grant No. hmz18 and funding by the DFG through the Emmy Noether Program under contract No. WE4425/1-1.

-
- [1] Henkel, M. *Conformal Invariance and Critical Phenomena* (Springer, Berlin/Heidelberg/New York, 1999).
- [2] Weigel, M. & Janke, W. Universal amplitudes in the finite-size scaling of three-dimensional spin models. *Phys. Rev. Lett.* **82**, 2318 (1999).
- [3] Young, A. P. (ed.) *Spin Glasses and Random Fields* (World Scientific, Singapore, 1997).
- [4] Cardy, J. Conformal invariance in percolation, self-avoiding walks, and related problems. *Ann. Henri Poincaré* **4**, 371–384–384 (2003).
- [5] Nienhuis, B. Coulomb gas formulation of two-dimensional phase transitions. In Domb, C. & Lebowitz, J. L. (eds.) *Phase Transitions and Critical Phenomena*, vol. 11, 1 (Academic Press, London, 1987).
- [6] Duplantier, B. Higher conformal multifractality. *J. Stat. Phys.* **110**, 691–738 (2003).
- [7] Bauer, M. & Bernard, D. 2d growth processes: SLE and loewner chains. *Phys. Rep.* **432**, 115–221 (2006).
- [8] Amoroso, C., Hartmann, A. K., Hastings, M. B. & Moore, M. A. Conformal invariance and stochastic loewner evolution processes in two-dimensional Ising spin glasses. *Phys. Rev. Lett.* **97**, 267202 (2006).
- [9] Bernard, D., Le Doussal, P. & Middleton, A. A. Possible description of domain walls in two-dimensional spin glasses by stochastic Loewner evolutions. *Phys. Rev. B* **76**, 020403 (2007).
- [10] Weigel, M. & Janke, W. Geometric and stochastic clusters of gravitating Potts models. *Phys. Lett. B* **639**, 373 (2006).
- [11] Jacobsen, J. L., Le Doussal, P., Picco, M., Santachiara, R. & Wiese, K. J. Critical interfaces in the random-bond Potts model. *Phys. Rev. Lett.* **102**, 070601 (2009).
- [12] Schwarz, K., Karrenbauer, A., Schehr, G. & Rieger, H. Domain walls and chaos in the disordered SOS model. *J. Stat. Mech. - Theory Exp.* P08022 (2009).
- [13] Nattermann, T. Theory of the random field Ising model. In Young, A. P. (ed.) *Spin Glasses and Random Fields*, 277 (World Scientific, 1997).
- [14] Stevenson, J. D., Walczak, A. M., Hall, R. W. & Wolyne, P. G. Constructing explicit magnetic analogies for the dynamics of glass forming liquids. *J. Chem. Phys.* **129**, 194505 (2008).
- [15] Feldman, D. E. Quasi-long range order in glass states of impure liquid crystals, magnets, and superconductors. *Int. J. Mod. Phys. B* **15**, 2945 (2001).
- [16] Imry, Y. & Ma, S. K. Random-field instability of the ordered state of continuous symmetry. *Phys. Rev. Lett.* **35**, 1399 (1975).
- [17] Binder, K. Random-field induced interface widths in ising systems. *Z. Phys. B* **50**, 343 (1983).
- [18] Aizenman, M. & Wehr, J. Rounding of first-order phase transitions in systems with quenched disorder. *Phys. Rev. Lett.* **62**, 2503 (1989).
- [19] Seppälä, E. T., Petäjä, V. & Alava, M. J. Disorder, order, and domain wall roughening in the two-dimensional random field Ising model. *Phys. Rev. E* **58**, R5217–R5220 (1998).
- [20] Seppälä, E. T. & Alava, M. J. Susceptibility and percolation in two-dimensional random field Ising magnets. *Phys. Rev. E* **63**, 066109 (2001).
- [21] Környei, L. & Iglói, F. Geometrical clusters in two-dimensional random-field ising models. *Phys. Rev. E* **75**, 011131 (2007).
- [22] Stevenson, J. D. & Weigel, M. Percolation and Schramm-Loewner evolution in the 2d random-field Ising model. *Comp. Phys. Comm.* **182**, 1879 (2011).
- [23] Kertész, J. Existence of weak singularities when going around the liquid-gas critical point. *Physica A* **161**, 58 (1989).
- [24] Anglès d’Auriac, J. C., Preissmann, M. & Rammal, R. The random field Ising model - algorithmic complexity and phase transition. *J. Physique Lett.* **46**, L173–L180 (1985).
- [25] Boykov, Y. & Kolmogorov, V. An experimental comparison of min-cut/max-flow algorithms for energy minimization in vision. *IEEE T. Pattern Anal.* **26**, 1124–1137 (2004).
- [26] Schramm, O. Scaling limits of loop-erased random walks and uniform spanning trees. *Israel J. Math.* **118**, 221–288 (2000).
- [27] Schramm, O. A percolation formula. *Electron. Comm. Probab.* **12**, 115 (2001).
- [28] Cardy, J. L. Critical percolation in finite geometries. *J. Phys. A - Math. Gen.* **25**, L201–L206 (1992).
- [29] Smirnov, S. Critical percolation in the plane: conformal invariance, Cardy’s formula, scaling limits. *Comptes Rendus L Acad. Sci. Ser. I - Math.* **333**, 239–244 (2001).
- [30] Kennedy, T. Computing the Loewner driving process of random curves in the half plane. *J. Stat. Phys.* **131**, 803–819 (2008).
- [31] James, F. *Statistical methods in experimental physics*, v2 (World Scientific, 2006).
- [32] Bastea, S. & Duxbury, P. M. Ground state structure of random magnets. *Phys. Rev. E* **58**, 4261–4265 (1998).
- [33] Risau-Gusman, S. & Romá, F. Fractal dimension of domain walls in the edwards-anderson spin glass model. *Phys. Rev. B* **77**, 134435 (2008).